



Article

Crystal Chemistry of Alkali–Aluminum–Iron Sulfates from the Burnt Mine Dumps of the Chelyabinsk Coal Basin, South Urals, Russia

Andrey A. Zolotarev ^{1,*} , Sergey V. Krivovichev ^{1,2} , Margarita S. Avdontceva ¹, Vladimir V. Shilovskikh ³, Mikhail A. Rassomakhin ⁴, Vasilij O. Yapaskurt ⁵ and Igor V. Pekov ⁵

¹ Department of Crystallography, Institute of Earth Sciences, St. Petersburg State University, University Emb. 7/9, 199034 St. Petersburg, Russia; s.krivovichev@spbu.ru (S.V.K.); margarita.avdontceva@spbu.ru (M.S.A.)

² Federal Research Center, Kola Science Center, Russian Academy of Sciences, Fersmana Str. 14, 184209 Apatity, Russia

³ Geomodel Research Centre, St. Petersburg State University, University Emb. 7/9, 199034 St. Petersburg, Russia; st036029@student.spbu.ru

⁴ South Urals Federal Research Center of Mineralogy and Geoecology of UB RAS, 456317 Miass, Russia; miha_rassomahin@mail.ru

⁵ Faculty of Geology, Moscow State University, 119991 Moscow, Russia; yvo72@geol.msu.ru (V.O.Y.); igorpekov@mail.ru (I.V.P.)

* Correspondence: a.zolotarev@spbu.ru; Tel.: +7-812-350-66-88

Received: 5 November 2020; Accepted: 20 November 2020; Published: 22 November 2020



Abstract: Technogenic steklite, $KAl(SO_4)_2$, and unnamed mineral phase $(K,Na)_3Na_3(Fe,Al)_2(SO_4)_6$ from burnt dumps of the Chelyabinsk Coal Basin have been investigated by single-crystal X-ray diffraction and electron microprobe analysis. Steklite is trigonal, space group $P\bar{3}$, $a = 4.7277(3)$, $c = 7.9871(5)$ Å, $V = 154.60(2)$ Å³. The crystal structure was refined to $R_1 = 0.026$ ($wR_2 = 0.068$). It is based upon the $[Al(SO_4)_2]^-$ layers formed by corner sharing of SO_4 tetrahedra and AlO_6 polyhedra. The anionic $[Al(SO_4)_2]^-$ layers are parallel to the (001) plane and linked via interlayer K^+ ions. The regular octahedral coordination of Al is observed that distinguishes technogenic steklite from that found in Tolbachik fumaroles. The $(K,Na)_3Na_3(Fe,Al)_2(SO_4)_6$ phase is trigonal, space group $R\bar{3}$, $a = 13.932(2)$, $c = 17.992(2)$ Å, $V = 3024.4(7)$ Å³, $R_1 = 0.073$ ($wR_2 = 0.108$). The crystal structure is based upon the anionic chains $[(Fe,Al)(SO_4)_3]^{3-}$ running parallel to the c axis and interconnected via K^+ and Na^+ ions. There are no known minerals or synthetic compounds isotypic to $(K,Na)_3Na_3(Fe,Al)_2(SO_4)_6$, due to the presence of separate K and Na sites in its structure.

Keywords: alkali–aluminum–iron sulfate; steklite; Chelyabinsk Coal Basin; burnt dump; anthropogenic (technogenic) mineralogy

1. Introduction

This study is a continuation of the series of our publications devoted to the specific features of the crystal chemistry of technogenic minerals from burnt dumps of the Chelyabinsk Coal Basin [1–5]. Here, we report, in detail, the features of two alkali-bearing Al–Fe sulfates crystallized from gaseous phases in high-temperature technogenic environments.

In general, sulfates constitute one of the most important classes of minerals which contains numerous species diverse from both chemical and structural points of view [6]. The technogenic sulfates formed at burning dumps of coal mines are close in their genetic features to purely natural sulfates crystallizing in oxidizing-type volcanic fumaroles (for recent discoveries, see [7–11]).

The first sulfate phase studied here is steklite, ideally $KAl(SO_4)_2$, which was originally reported by B.V. Chesnokov in 1991 as a new mineral species from burnt dumps of coal mines of the Chelyabinsk Coal Basin, South Urals, Russia [12,13]. The crystals of the technogenic mineral phase were visually very similar to glass plates, which inspired its name “steklite” from the Russian word “steklo”, which means “glass”. Like many other new phases from the burnt coal dumps of the Chelyabinsk Coal Basin, steklite was not accepted by the International Mineralogical Association (IMA) as a valid mineral species at the time, due to its technogenic origin. Later, steklite was found in sublimates of the Yadovitaya (Poisonous) fumarole at the second scoria cone of the Northern Breach of the Great Fissure Tolbachik Eruption at the Tolbachik volcano (Kamchatka Peninsula, Russia) and was approved by the IMA as a valid mineral species [14]. Even before the official approval of steklite in 2013, the $KAl(SO_4)_2$ phase was repeatedly reported from various natural and anthropogenic environments: the volcanic exhalations at the Showashinzan lava dome, Hokkaido, Japan [15]; fumaroles of two active volcanoes in Central America, namely Izalco in El Salvador and Santiagito in Guatemala [16]; high-temperature products of coal fire at the anthracite mines in eastern Pennsylvania, USA [17]; exhalations of fires in mine dumps at Radvanice, Czech Republic [18], and at Marcel, Poland [19]. The Raman spectroscopic study of synthetic $KAl(SO_4)_2$ was performed by Košek et al. [20].

Another sulfate reported here is a new mineral phase with the simplified formula $(K,Na)_3Na_3(Fe,Al)_2(SO_4)_6$, found in association with the abovementioned technogenic steklite. This phase has not been previously described in the literature. It is related to some known natural sulfates, especially aluminocoquimbite and pyracmonite (see details below).

According to the current recommendations of the Commission on New Minerals, Nomenclature and Classification (CNMNC) of the IMA, the newly formed minerals found in burnt coal dumps can be considered as valid mineral species, assuming that “the fire occurred as a result of natural events (self-ignition or lightning) and, beyond a shadow of doubt, was not of anthropogenic origin” [21]. Therefore, the new $(K,Na)_3Na_3(Fe,Al)_2(SO_4)_6$ phase reported herein can be considered as a potential separate mineral species, despite its technogenic origin in burnt mine dumps of the Chelyabinsk coal basin. In the following we shall call both the new phase and steklite from the Kopeisk dumps “technogenic”, in order to distinguish their origin from the mineral phases found in volcanic fumarolic environments.

2. Materials and Methods

2.1. Materials

The samples of steklite (Figure 1) studied by us are of technogenic origin and were selected from the collection of Boris V. Chesnokov currently deposited at the Natural Science Museum of the Ilmen State Reserve (Miass, Russia). The sample originates from the coal dump of the mine No. 47 in the city of Kopeisk, Chelyabinsk area, Southern Urals, Russia [13], where it was found as transparent colorless hexagonal lamellar crystals with the average size of 0.3–0.5 mm.

The $(K,Na)_3Na_3(Fe,Al)_2(SO_4)_6$ phase occurs together with steklite. It is transparent colorless with a characteristic reddish hue and forms platy crystals up to 0.1 mm. According to Chesnokov et al. [13], steklite and $(K,Na)_3Na_3(Fe,Al)_2(SO_4)_6$ are high-temperature (650–750 °C) pneumatolytic compounds related to sintered rocks.

2.2. Chemical Composition

The chemical composition of technogenic steklite was determined using a Hitachi S-3400N equipped with Oxford X-Max 20 energy dispersive X-ray spectrometer at the Resource Centre “Geomodel” of St. Petersburg State University. The spectra were processed automatically using the AzTec Energy software package using the TrueQ technique. The electron beam accelerating voltage was 20 kV and 1 nA current was used. The X-ray acquisition time was 60 s both in spot mode and small area scanning. Quantification of elemental compositions was conducted using standard samples of natural and synthetic compounds ($NaAlSi_3O_8$ for Na and Al, $KAlSi_3O_8$ for K, $CaSiO_3$ for Si and

O, FeS₂ for Fe, CaSO₄ for S). The average composition (wt.%) is Na₂O 0.26, K₂O 17.08, Al₂O₃ 21.65, Fe₂O₃ 2.52, SiO₂ 0.21, SO₃ 58.75; total 100.47. The empirical formula calculated based on 8 oxygen atoms is (K_{0.94}Na_{0.02})_{Σ0.96}(Al_{1.10}Fe³⁺_{0.08}Si_{0.01})_{Σ1.19}S_{1.91}O₈, and the idealized formula is KAl(SO₄)₂.

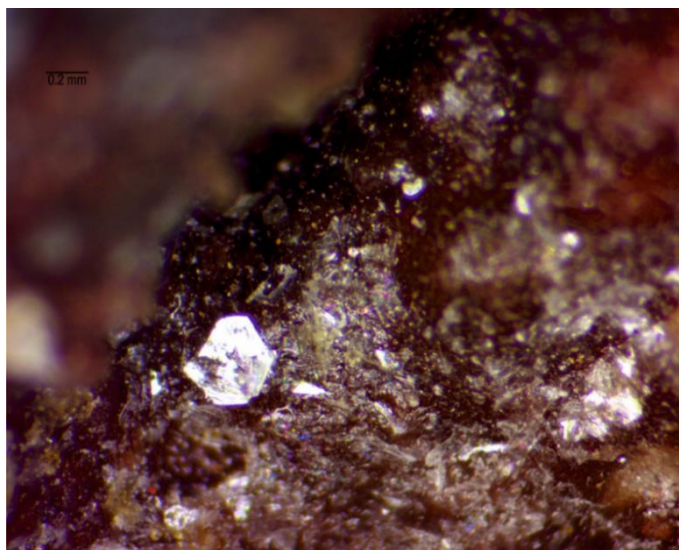


Figure 1. The colorless platelets of steklite on a sintered rock from the burnt dump of the Mine No. 47, Kopeisk, South Urals.

The chemical composition of the (K,Na)₃Na₃(Fe,Al)₂(SO₄)₆ phase was determined on a Jeol JSM-6480LV scanning electron microscope equipped with an INCA-Wave 500 wavelength-dispersive spectrometer (Laboratory of Analytical Techniques of High Spatial Resolution, Dept. of Petrology, Moscow State University), with an acceleration voltage of 20 kV, a beam current of 20 nA, and a 3 μm beam diameter. The following standards were used: albite (Na), microcline (K), diopside (Ca, Mg), Mn (Mn), Al₂O₃ (Al), magnetite (Fe), and SrSO₄ (S). The average composition (wt.%) is Na₂O 15.09, K₂O 10.90, CaO 0.12, MgO 0.10, MnO 0.05, Al₂O₃ 5.07, Fe₂O₃ 10.29, SO₃ 57.25, total 98.87. The empirical formula calculated based on 24 oxygen atoms is (K_{1.95}Na_{1.05})_{Σ3}(Na_{3.05}Ca_{0.02})_{Σ3.07}(Fe³⁺_{1.08}Al_{0.84}Mg_{0.02}Mn_{0.01})_{Σ1.95}S_{6.02}O₂₄.

2.3. Single-Crystal X-ray Diffraction

Single-crystal X-ray diffraction study of steklite and (K,Na)₃Na₃(Fe,Al)₂(SO₄)₆ from Kopeisk was performed at the X-ray Diffraction Resource Centre of St. Petersburg State University. In the case of steklite, a Bruker Kappa APEX DUO diffractometer operated at 45 kV and 0.6 mA and equipped with a CCD area detector was used for data collection. The study was done by means of monochromatic MoKα radiation (λ = 0.71073 Å), frame widths of 0.5° in ω, and 10 s counting time for each frame. The intensity data were reduced and corrected for Lorentz, polarization, and background effects using Bruker software APEX2 [22]. A semiempirical absorption-correction based upon the intensities of equivalent reflections was applied [23]. The (K,Na)₃Na₃(Fe,Al)₂(SO₄)₆ phase was studied on a STOE IPDS II diffractometer. More than half of the diffraction sphere were collected using MoKα radiation and scanning along ω with a step of 2° and 3 min exposition. The distance of the crystal detector was chosen equal to 100 mm. The numerical absorption correction based on measured crystal faces was applied using the X-RED [24] and X-SHAPE [25] programs.

The crystal structure of steklite was solved by direct methods and refined in the space group $P\bar{3}$ to $R_1 = 0.026$ ($wR_2 = 0.068$) for 565 unique observed reflections with $I \geq 2\sigma(I)$ using ShelX program package [26] within the Olex2 shell [27]. The crystal structure of (K,Na)₃Na₃(Fe,Al)₂(SO₄)₆ was solved and refined in the space group $R\bar{3}$ to $R_1 = 0.073$ ($wR_2 = 0.108$) for 1200 unique observed reflections with $I \geq 2\sigma(I)$ using ShelX program package [26].

Crystal data, data collection information, and structure refinement details for both phases are given in Table 1; atom coordinates and displacement parameters are in Tables 2 and 3, and selected interatomic distances are in Table 4. Crystallographic data have been deposited at Cambridge Crystallographic Data Centre (2,042,224 for steklite; 2,042,223 for $(\text{K,Na})_3\text{Na}_3(\text{Fe,Al})_2(\text{SO}_4)_6$) (also see Supplementary Materials).

Table 1. Crystal data and structure refinement parameters for both studied sulfates.

Phase	Steklite $\text{KAl}(\text{SO}_4)_2$	$(\text{K,Na})_3\text{Na}_3(\text{Fe,Al})_2(\text{SO}_4)_6$
Crystal system	trigonal	trigonal
Space group	$P\bar{3}$	$R\bar{3}$
a , Å	4.7277(3)	13.932(2)
c , Å	7.9871(5)	17.992(2)
V , Å ³	154.60(2)	3024.4(7)
Z	1	6
D_{calc} , g cm ⁻³	2.801	2.784
μ , mm ⁻¹	1.873	2.354
$F(000)$	129.0	2497.0
Radiation	MoK α ($\lambda = 0.71073$)	MoK α ($\lambda = 0.71073$)
2 Θ range for data collection, °	5.1 to 81.742	4.06 to 53.98
Index ranges	$-8 \leq h \leq 5, -7 \leq k \leq 8, -14 \leq l \leq 14$	$-17 \leq h \leq 17, -17 \leq k \leq 17, -19 \leq l \leq 22$
Reflections collected	1948	6934
Independent reflections	650 [$R_{\text{int}} = 0.0208$]	1466 [$R_{\text{int}} = 0.088$]
Data/restraints/parameters	650/0/21	1466/0/116
Goodness-of-fit on F^2	1.107	1.184
Final R indexes [$I \geq 2\sigma(I)$]	$R_1 = 0.0262, wR_2 = 0.0680$	$R_1 = 0.0728, wR_2 = 0.1075$
Final R indexes [all data]	$R_1 = 0.0314, wR_2 = 0.0712$	$R_1 = 0.0914, wR_2 = 0.1130$
Largest diff. peak/hole/e Å ⁻³	1.09/−0.42	0.76/−0.56

Table 2. Atomic fractional coordinates, site occupancies, bond valence sums, and equivalent displacement parameters (Å²) for atoms of both studied sulfates.

Atom	x	y	z	U_{eq}	Occupancy	BVS *
Steklite $\text{KAl}(\text{SO}_4)_2$						
K	0	0	0	0.0235(1)	K	1.09
Al	0	0	$\frac{1}{2}$	0.0089(2)	Al _{0.90} Fe _{0.10}	3.15
S	$\frac{1}{3}$	$\frac{2}{3}$	0.29602(4)	0.0092(1)	S	6.06
O1	$\frac{1}{3}$	$\frac{2}{3}$	0.1153(1)	0.0188(3)	O	1.76
O2	0.2805(2)	0.9312(2)	0.35885(9)	0.0133(1)	O	2.06
$(\text{K,Na})_3\text{Na}_3(\text{Fe,Al})_2(\text{SO}_4)_6$						
Fe1	0	0	0	0.0075(4)	Fe _{0.78} Al _{0.22}	2.92
Fe2	$\frac{1}{3}$	$\frac{2}{3}$	−0.08861(9)	0.0083(3)	Fe _{0.66} Al _{0.34}	3.06
Fe3	$\frac{1}{3}$	$\frac{2}{3}$	$\frac{1}{6}$	0.0090(4)	Fe _{0.78} Al _{0.22}	2.95
S1	0.31822(11)	0.49209(11)	0.03634(7)	0.0150(3)	S	6.08
S2	0.04720(11)	0.19237(10)	0.12854(7)	0.0142(3)	S	6.04
K	0.29774(13)	0.22033(12)	0.07635(9)	0.0265(4)	K _{0.73} Na _{0.27}	0.94
Na	0.4390(2)	0.3950(2)	−0.0843(2)	0.0308(6)	Na	1.06
O1	0.0604(4)	0.1398(3)	0.0596(2)	0.0237(9)	O	2.02
O2	0.1557(3)	0.2626(4)	0.1594(2)	0.0235(9)	O	2.05
O3	0.4613(3)	0.6927(3)	−0.1522(2)	0.0199(8)	O	1.97
O4	0.2515(4)	0.2621(4)	−0.1097(3)	0.029(1)	O	2.01
O5	0.3590(4)	0.5619(4)	0.1053(2)	0.0243(9)	O	1.99
O6	0.3705(4)	0.4246(4)	0.0351(2)	0.0253(9)	O	2.05
O7	0.1989(3)	0.4289(4)	0.0351(3)	0.0259(9)	O	2.02
O8	0.3626(4)	0.5673(4)	−0.0286(2)	0.0255(9)	O	2.00

* Bond valence parameters are taken according to [28].

Table 3. Anisotropic displacement parameters of atoms (\AA^2) for the crystal structures of steklite and $(\text{K,Na})_3\text{Na}_3(\text{Fe,Al})_2(\text{SO}_4)_6$.

Atom	U_{11}	U_{22}	U_{33}	U_{23}	U_{13}	U_{12}
Steklite $\text{KAl}(\text{SO}_4)_2$						
K	0.0212(2)	$=U_{11}$	0.0280(2)	0	0	0.01062(9)
S	0.0076(1)	$=U_{11}$	0.0123(1)	0	0	0.00380(6)
Al	0.0065(2)	$=U_{11}$	0.0136(3)	0	0	0.033(1)
O1	0.0220(4)	$=U_{11}$	0.0124(4)	0	0	0.0110(2)
O2	0.0107(3)	0.0087(3)	0.0216(3)	−0.0002(2)	0.0020(2)	0.0056(2)
$(\text{K,Na})_3\text{Na}_3(\text{Fe,Al})_2(\text{SO}_4)_6$						
Fe1	0.0090(5)	$=U_{11}$	0.0045(9)	0	0	0.0045(3)
Fe2	0.0103(4)	$=U_{11}$	0.0041(6)	0	0	0.0052(2)
Fe3	0.0107(6)	$=U_{11}$	0.0056(9)	0	0	0.0053(3)
S1	0.0155(6)	0.0143(6)	0.0151(7)	−0.0001(5)	−0.0001(5)	0.0073(5)
S2	0.0155(6)	0.0127(6)	0.0143(6)	−0.0013(5)	−0.0003(5)	0.0069(5)
K	0.0287(8)	0.0187(7)	0.0335(9)	0.0041(6)	0.0114(7)	0.0129(6)
Na	0.0258(13)	0.0296(13)	0.0348(14)	0.0109(12)	−0.0027(11)	0.0121(11)
O1	0.029(2)	0.018(2)	0.020(2)	−0.0016(17)	0.0008(18)	0.0081(18)
O2	0.021(2)	0.021(2)	0.021(2)	−0.0080(17)	−0.0043(17)	0.0055(17)
O3	0.021(2)	0.020(2)	0.019(2)	−0.0020(16)	0.0030(16)	0.0103(17)
O4	0.026(2)	0.018(2)	0.042(3)	−0.0081(19)	−0.009(2)	0.0086(18)
O5	0.028(2)	0.030(2)	0.019(2)	−0.0091(18)	−0.0046(18)	0.0184(19)
O6	0.033(2)	0.025(2)	0.027(2)	−0.0024(18)	−0.001(2)	0.021(2)
O7	0.018(2)	0.024(2)	0.029(2)	−0.0041(19)	−0.0030(19)	0.0055(18)
O8	0.027(2)	0.028(2)	0.022(2)	0.0083(19)	0.0050(18)	0.0141(19)

Table 4. Selected bond lengths (\AA) in crystal structures of steklite and $(\text{K,Na})_3\text{Na}_3(\text{Fe,Al})_2(\text{SO}_4)_6$.

Steklite $\text{KAl}(\text{SO}_4)_2$					
K-O2	3.2421(7) ×6	S-O2	1.4799(7) ×3	Al-O2	1.8888(7) ×6
K-O1	2.8808(4) ×6	S-O1	1.4431(11)		
<K-O>	3.0614	<S-O>	1.4707		
$(\text{K,Na})_3\text{Na}_3(\text{Fe,Al})_2(\text{SO}_4)_6$					
Fe1-O1	2.004(4) ×6	S2-O2	1.439(4)	K-O6	2.606(5)
		S2-O4	1.450(4)	K-O7	2.671(5)
Fe2-O8	1.953(4) ×3	S2-O3	1.495(4)	K-O2	2.768(5)
Fe2-O3	1.993(4) ×3	S2-O1	1.497(4)	K-O4	2.774(5)
<Fe2-O>	1.973	<S2-O>	1.470	K-O1	2.928(5)
				K-O4	3.025(5)
Fe3-O5	2.000(4) ×6	Na-O2	2.277(5)	K-O3	3.174(4)
		Na-O4	2.373(5)	K-O1	3.219(5)
S1-O7	1.441(4)	Na-O7	2.400(5)	K-O3	3.245(4)
S1-O6	1.449(4)	Na-O6	2.467(5)	<K-O>	2.934
S1-O8	1.482(4)	Na-O5	2.594(5)		
S1-O5	1.501(4)	Na-O6	2.733(5)		
<S1-O>	1.468	<Na-O>	2.474		

3. Results

The crystal structure of synthetic $\text{KAl}(\text{SO}_4)_2$ was first reported in 1970 [29] as based upon the $[\text{Al}(\text{SO}_4)_2]^-$ layers formed by corner sharing of SO_4 tetrahedra and AlO_6 polyhedra (Figure 2). The anionic $[\text{Al}(\text{SO}_4)_2]^-$ layers are parallel to the (001) plane and linked via interlayer K^+ ions. The layer topology in steklite can be described using the 2D graph representation, where black and white vertices symbolize the Al and S polyhedra, respectively (Figure 3). The observed topology is identical to that of the $[\text{Fe}(\text{SO}_4)_2]^-$ layers in yavapaiite, $\text{KFe}(\text{SO}_4)_2$ [30,31], and the $[\text{Mg}(\text{PO}_4)_2]^{4-}$ layers in brianite,

$\text{Na}_2\text{CaMg}(\text{PO}_4)_2$ [32], as well as to the similar anionic layers in a number of synthetic compounds [33]. The average $\langle\text{S-O}\rangle$ bond length in sulfate tetrahedra in steklite is 1.471 \AA , with the S–O distances for the O atoms bridging between sulfate tetrahedra with AlO_6 polyhedra (1.478 \AA) essentially longer than that for the terminal O atoms (1.443 \AA) (Table 4). The Al atom has an octahedral coordination with the $\langle\text{Al-O}\rangle$ bond length equal to 1.889 \AA (see Discussion for more details). The interlayer K^+ cations are coordinated by 12 oxygen atoms with the $\langle\text{K-O}\rangle$ bond length equal to 3.061 \AA (Figure 4b).

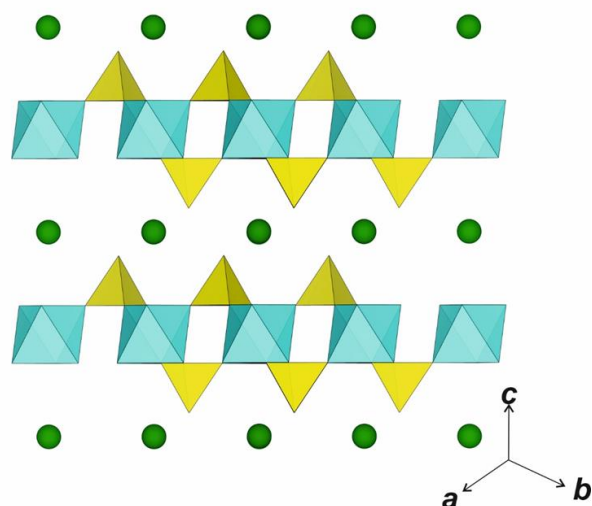


Figure 2. The crystal structure of steklite, $\text{KAl}(\text{SO}_4)_2$. SO_4 tetrahedra are yellow, AlO_6 octahedra are blue, and K atoms are green circles.

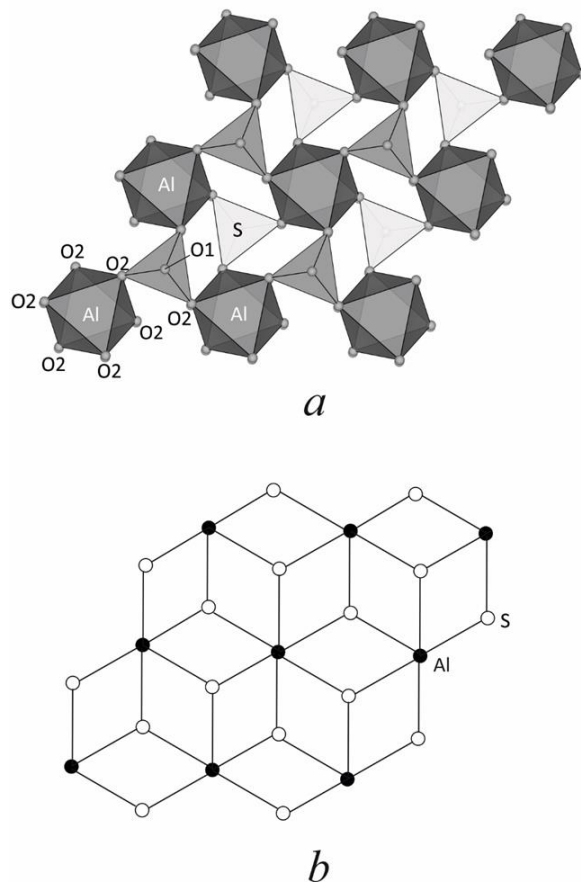


Figure 3. (a) The anionic $[\text{Al}(\text{SO}_4)_2]^-$ layer in steklite; (b) its 2D graph.

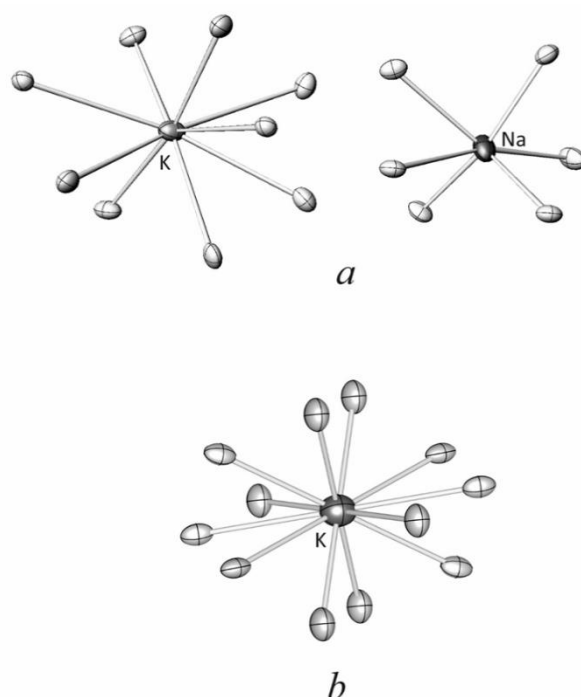


Figure 4. (a) The nine-coordinated K and six-coordinated Na sites in the crystal structure of $(\text{K,Na})_3\text{Na}_3(\text{Fe,Al})_2(\text{SO}_4)_6$; (b) the twelve-coordinated K site in the crystal structure of steklite, $\text{KAl}(\text{SO}_4)_2$.

In the crystal structure of $(\text{K,Na})_3\text{Na}_3(\text{Fe,Al})_2(\text{SO}_4)_6$, there are three symmetrically independent sites with octahedral coordination. All of them are predominantly occupied by Fe^{3+} with some amount of Al (Table 2). The average interatomic cation–anion distances for these sites approximately correlate with the amount of Al in these positions. Two crystallographic positions of S are in tetrahedral coordination; the average $\langle\text{S-O}\rangle$ bond lengths are 1.468 and 1.470 Å for S1 and S2, respectively. There are two sites occupied by the Na^+ and K^+ cations. The 9-coordinated K site (Figure 4a) contains mainly K, with the rather high Na content (27%) reflected in the noticeable shortening of the K–O bond lengths compared to pure K. The Na site is fully occupied by sodium and has a strongly distorted octahedral coordination (Figure 4a).

The projection of the crystal structure of $(\text{K,Na})_3\text{Na}_3(\text{Fe,Al})_2(\text{SO}_4)_6$ phase is shown in Figure 5. It is based upon the anionic chains $[(\text{Fe,Al})(\text{SO}_4)_3]^{3-}$, running parallel to the c axis and interconnected via K^+ and Na^+ ions. Within the chains, each $[(\text{Fe,Al})\text{O}_6]$ octahedron is corner-linked to six adjacent (SO_4) tetrahedra, while only two O atoms of each tetrahedron are bridging; that is, they form the S–O–Fe bonds (Figure 6a). The S–O bond lengths for the bridging O atoms are longer (1.482–1.501 Å) than those for terminal oxygen atoms (1.439–1.450 Å), in agreement with the similar observation for steklite. The calculated crystal chemical formula of $(\text{K,Na})_3\text{Na}_3(\text{Fe,Al})_2(\text{SO}_4)_6$ phase can be represented as $(\text{K}_{2.19}\text{Na}_{0.81})_{\Sigma 3}\text{Na}_3(\text{Fe}^{3+}_{1.44}\text{Al}_{0.56})_{\Sigma 2}(\text{SO}_4)_6$, which is generally in good agreement with the empirical formula, taking into account variations in the composition of the studied phase.

The average $\langle\text{S-O}\rangle$ bond lengths for both sulfates studied herein are consistent with the average value of 1.473 Å, determined for sulfate minerals by Hawthorne et al. [6]. In both phases, the S–O bond lengths for bridging O atoms are longer than those for terminal oxygen atoms, which is typical for heteropolyhedral complexes with tetrahedral oxoanions and is widely manifested, for example, in uranyl salts [34].

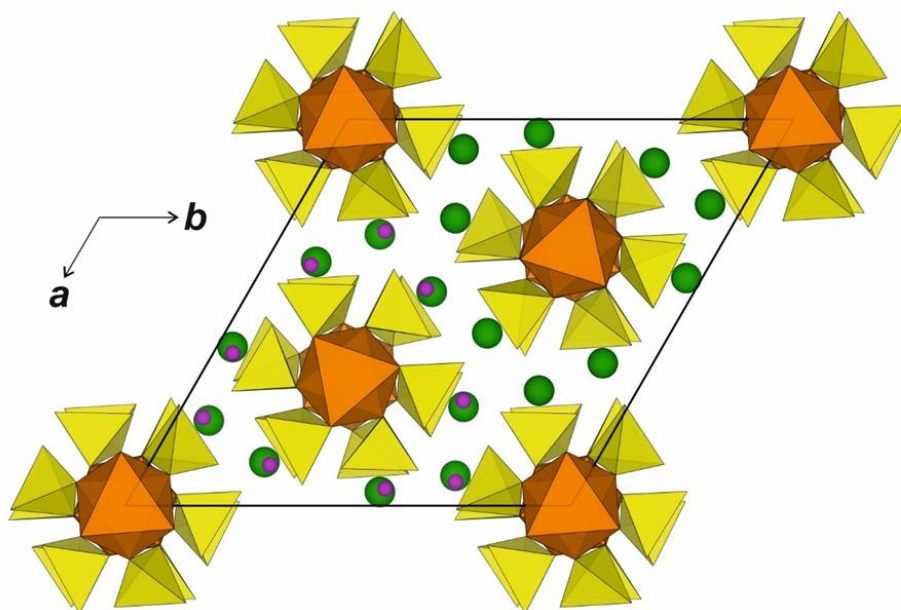


Figure 5. The crystal structure of $(\text{K,Na})_3\text{Na}_3(\text{Fe,Al})_2(\text{SO}_4)_6$: projection onto the (001) plane. SO_4 tetrahedra are yellow, FeO_6 octahedra are brown, K and Na atoms are green and purple circles, respectively.

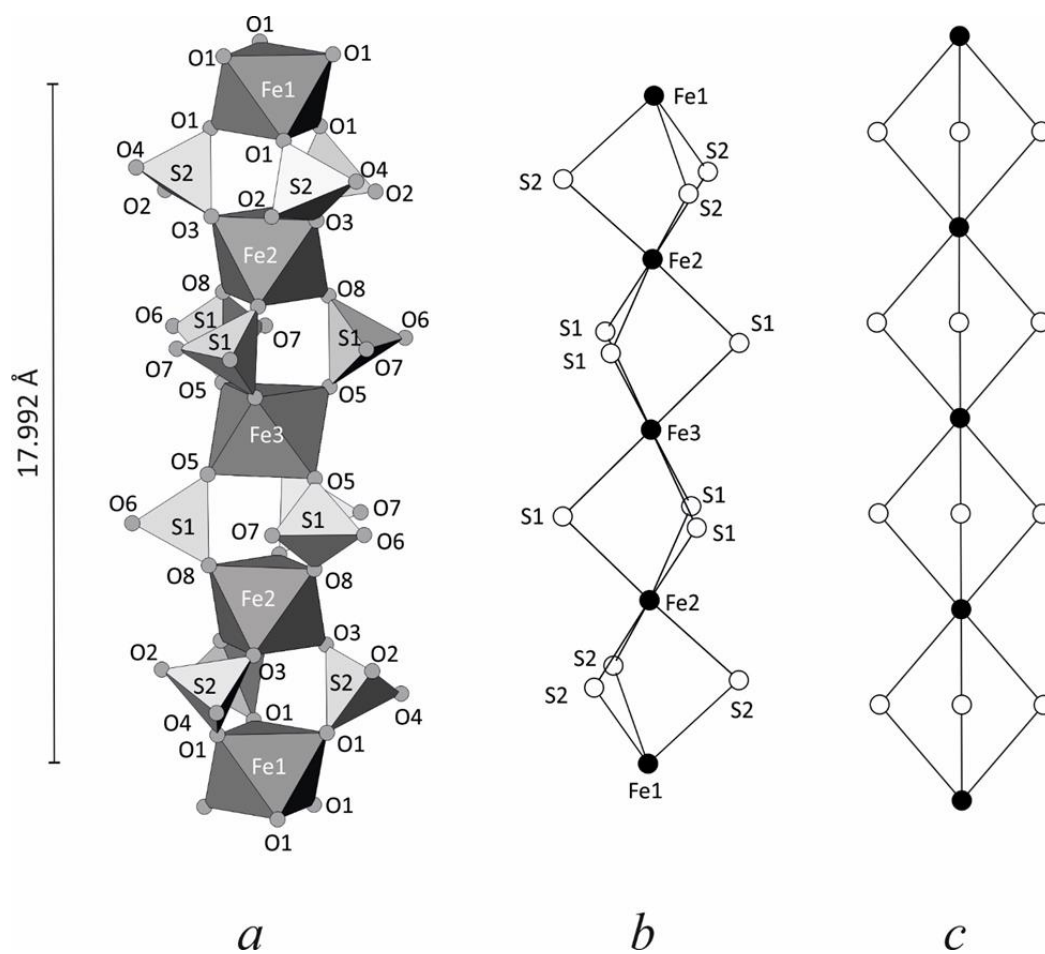


Figure 6. (a) The anionic $[(\text{Fe,Al})(\text{SO}_4)_3]^{3-}$ chain in $(\text{K,Na})_3\text{Na}_3(\text{Fe,Al})_2(\text{SO}_4)_6$, (b) its 1D graph, and (c) the idealized graph with 6-connected black and 2-connected white vertices.

4. Discussion

The most interesting aspect of the crystal structure of steklite studied here is related to the shape of the AlO_6 polyhedra. In general, the AlO_6 coordination polyhedron in $\text{KAl}(\text{SO}_4)_2$ may theoretically adopt either trigonal prismatic or octahedral geometry. For the $\text{KM}(\text{SO}_4)_2$ compounds (where M is a trivalent cation), the octahedral AlO_6 configuration was reported for the $P\bar{3}$ space group, and the trigonal prismatic configuration was observed for the $P312$ space group [33]. West et al. [35] indicated that synthetic $\text{KAl}(\text{SO}_4)_2$ crystallizes in the $P\bar{3}$ space group with the octahedral coordination of Al and disorder in the stacking of adjacent layers due to the rotation of polyhedra within the layers around the direction parallel to the c axis. However, Murashko et al. [14] described natural, fumarolic steklite from the Tolbachik volcano with coordination polyhedron of Al intermediate in a shape between a trigonal prism and octahedron with the rotation angle between the upper and lower triangular bases of about 10° (it is equal to 0 and 30° for a trigonal prism and an octahedron, respectively). In the case of fumarolic steklite, no disorder induced by the rotation of AlO_6 polyhedra was detected, and the crystal structure is well described by the $P312$ space group. In the case of technogenic steklite studied here, the regular octahedral coordination of Al was observed (space group $P\bar{3}$) that distinguishes Kopeisk steklite from that found in Tolbachik fumaroles. The origin of different AlO_6 configurations in steklite from different occurrences requires additional comment. The difference in unit cell volumes between Tolbachik and Kopeisk samples of steklite is in fact negligible (154.76 vs. 154.60 \AA^3 , respectively) and does not allow considering them as temperature-related. According to Murashko et al. [14], the temperature of formation of steklite in fumaroles cannot be determined reliably; the possible temperature range is $150\text{--}340^\circ\text{C}$. For the Kopeisk sulfates, Chesnokov et al. [13] assigned the crystallization temperature of $650\text{--}750^\circ\text{C}$, i.e., sufficiently higher than that in volcanic fumaroles. There is a general agreement that the symmetry and shape of local configurations in crystals tends to be higher with the increase of temperature [36]. This agrees well with the possible higher-temperature origin of the Kopeisk steklite compared to the Tolbachik sample, since the symmetry of an octahedron ($m\text{--}3m$; point group order = 48) is higher than that of a trigonal prism ($\text{--}62m$; point group order = 12). However, the problem is far from being clear and needs further experimental investigation.

The topology of the octahedral–tetrahedral chains in $(\text{K,Na})_3\text{Na}_3(\text{Fe,Al})_2(\text{SO}_4)_6$ can be described using the 1D graph shown in Figure 6b, where black and white vertices symbolize octahedra and tetrahedra, respectively. Figure 6c shows an idealized graph in which each black vertex is 6-connected, and each white vertex is 2-connected. The topology shown in Figure 6c is quite common for the crystal structures of oxosalts of metals in octahedral coordination [33]. Among minerals, it was observed in the crystal structures of kaatialaite, $\text{Fe}(\text{H}_2\text{AsO}_4)_3(\text{H}_2\text{O})_5$ [37], and ferrinatrite, $\text{Na}_3[\text{Fe}^{3+}(\text{SO}_4)_3](\text{H}_2\text{O})_3$ [38,39], as well as in fumarolic minerals such as aluminocoquimbite, $\text{AlFe}(\text{SO}_4)_3(\text{H}_2\text{O})_9$ [40], and pyracmonite, $(\text{NH}_4)_3\text{Fe}(\text{SO}_4)_3$ [41]. However, none of these minerals is isotypic to $(\text{K,Na})_3\text{Na}_3(\text{Fe,Al})_2(\text{SO}_4)_6$ due to the presence of separate K and Na sites in its structure. Ferrinatrite, aluminocoquimbite, and pyracmonite were found in the fumaroles of the La Fossa Crater (Vulcano Island, Sicily, Italy), which indicates the possibility of the formation of $(\text{K,Na})_3\text{Na}_3(\text{Fe,Al})_2(\text{SO}_4)_6$ under natural conditions during crystallization from high-temperature volcanic gases.

According to the current recommendations of the Commission on New Minerals, Nomenclature and Classification (CNMNC) of the IMA, the newly formed minerals found in burnt coal dumps can be considered as valid mineral species, assuming that “the fire occurred as a result of natural events (self-ignition or lightning) and, beyond a shadow of doubt, was not of anthropogenic origin” [21]. Therefore, the new $(\text{K,Na})_3\text{Na}_3(\text{Fe,Al})_2(\text{SO}_4)_6$ phase reported herein can be considered as a separate mineral species, despite its technogenic origin in burnt mine dumps of the Chelyabinsk coal basin.

Supplementary Materials: The following are available online at <http://www.mdpi.com/2073-4352/10/11/1062/s1>, $\text{KAl}(\text{SO}_4)_2$.CIF: Crystallographic Information file (CIF) for the crystal structure of $\text{KAl}(\text{SO}_4)_2$, $(\text{K,Na})_3\text{Na}_3(\text{Fe,Al})_2(\text{SO}_4)_6$.CIF: Crystallographic Information file (CIF) for the crystal structure of $(\text{K,Na})_3\text{Na}_3(\text{Fe,Al})_2(\text{SO}_4)_6$.

Author Contributions: Conceptualization, A.A.Z. and S.V.K.; Methodology, A.A.Z. and S.V.K.; Investigation, A.A.Z., S.V.K., M.S.A., M.A.R., V.V.S., I.V.P., V.O.Y.; Writing—Original Draft Preparation, A.A.Z. and S.V.K.; Writing—Review & Editing, S.V.K., I.V.P.; Visualization, A.A.Z. and S.V.K. All authors have read and agreed to the published version of the manuscript.

Funding: This research was funded by the Russian Foundation for Basic Research (electron probe microanalysis, single crystal X-ray diffraction; grant No. 19-05-00628) and by the President of Russian Federation grant for leading scientific schools (the theoretical crystal chemical analysis; grant No. NSh-2526.2020.5).

Acknowledgments: The X-ray diffraction studies were performed in the X-ray Diffraction Resource Centre of St. Petersburg State University. The chemical analytical studies were done in “Geomodel” Resource Centre of St. Petersburg State University.

Conflicts of Interest: The authors declare no conflict of interest.

References

1. Krivovichev, S.V.; Shcherbakova, E.P.; Nishanbaev, T.P. The crystal structure of β - $\text{CaMg}_2(\text{SO}_4)_3$, a mineral phase from coal dumps of the Chelyabinsk coal basin, Russia. *Can. Mineral.* **2010**, *48*, 1469–1475. [[CrossRef](#)]
2. Krivovichev, S.V.; Shcherbakova, E.P.; Nishanbaev, T.P. The crystal structure of svyatoslavite and evolution of complexity during crystallization of a $\text{CaAl}_2\text{Si}_2\text{O}_8$ melt: A structural automata description. *Can. Mineral.* **2012**, *50*, 585–592. [[CrossRef](#)]
3. Zolotarev, A.A.; Krivovichev, S.V.; Panikorovskii, T.L.; Gurzhiy, V.V.; Bocharov, V.N.; Rassomakhin, M.A. Dmisteinbergite, $\text{CaAl}_2\text{Si}_2\text{O}_8$, a metastable polymorph of anorthite: Crystal-structure and Raman spectroscopic study of the holotype specimen. *Minerals* **2019**, *9*, 570. [[CrossRef](#)]
4. Zolotarev, A.A.; Zhitova, E.S.; Krzhizhanovskaya, M.G.; Rassomakhin, M.A.; Shilovskikh, V.V.; Krivovichev, S.V. Crystal chemistry and high-temperature behaviour of ammonium phases $\text{NH}_4\text{MgCl}_3 \cdot 6\text{H}_2\text{O}$ and $(\text{NH}_4)_2\text{Fe}^{3+}\text{Cl}_5 \cdot \text{H}_2\text{O}$ from the burned dumps of the Chelyabinsk coal basin. *Minerals* **2019**, *9*, 486. [[CrossRef](#)]
5. Zolotarev, A.A.; Krivovichev, S.V.; Avdontceva, M.S.; Zhitova, E.S.; Pekov, I.V.; Shchipalkina, N.V. Crystal chemistry of technogenic SFCA from burned dumps of the Chelyabinsk coal basin. *Crystallogr. Rep.* **2021**, in press.
6. Hawthorne, F.C.; Krivovichev, S.V.; Burns, P.C. The crystal chemistry of sulfate minerals. *Rev. Miner. Geochem.* **2000**, *40*, 1–112. [[CrossRef](#)]
7. Pekov, I.V.; Shchipalkina, N.V.; Zubkova, N.V.; Gurzhiy, V.V.; Agakhanov, A.A.; Belakovskiy, D.I.; Chukanov, N.V.; Lykova, I.S.; Vlgasina, M.F.; Koshlyakova, N.N.; et al. Alkali sulfates with apththalite-like structures from fumaroles of the Tolbachik volcano, Kamchatka, Russia. I. Metathenardite, a natural high-temperature modification of Na_2SO_4 . *Can. Mineral.* **2019**, *57*, 885–901. [[CrossRef](#)]
8. Pekov, I.V.; Agakhanov, A.A.; Zubkova, N.V.; Koshlyakova, N.V.; Shchipalkina, N.V.; Sandalov, F.D.; Yapaskurt, V.O.; Turchkova, A.G.; Sidorov, E.G. Oxidizing-type fumaroles of the Tolbachik Volcano, a mineralogical and geochemical unique. *Russ. Geol. Geophys.* **2020**, *61*, 675–688. [[CrossRef](#)]
9. Filatov, S.K.; Shablinskii, A.P.; Vergasova, L.P.; Saprikina, O.Y.; Bubnova, R.S.; Moskaleva, S.V.; Belousov, A.B. Belomarinaite $\text{KNa}(\text{SO}_4)$: A new sulfate from 2012–2013 Tolbachik Fissure eruption, Kamchatka Peninsula, Russia. *Mineral. Mag.* **2019**, *83*, 569–575. [[CrossRef](#)]
10. Nazarchuk, E.V.; Siidra, O.I.; Nekrasova, D.O.; Shilovskikh, V.V.; Borisov, A.S.; Avdontseva, E.Y. Glikinite, $\text{Zn}_3\text{O}(\text{SO}_4)_2$, a new anhydrous zinc oxysulfate mineral structurally based on OZn_4 tetrahedra. *Mineral. Mag.* **2020**, *84*, 563–567. [[CrossRef](#)]
11. Shchipalkina, N.V.; Pekov, I.V.; Chukanov, N.V.; Belakovskiy, D.I.; Zubkova, N.V.; Koshlyakova, N.N.; Britvin, S.N.; Sidorov, E.G. Alkali sulfates with apththalite-like structures from fumaroles of the Tolbachik volcano, Kamchatka, Russia. II. A new mineral, natroapththalite, and new data on belomarinaite. *Can. Mineral.* **2020**, *58*, 167–181. [[CrossRef](#)]
12. Chesnokov, B.V.; Bazhenova, L.F.; Bushmakina, A.F.; Kotlyarov, V.A.; Belogub, E.V. New minerals from burnt dumps of the Chelyabinsk coal basin (communication seven). *Ural. Mineral. Sbornik* **1995**, *4*, 3–28. (In Russian)
13. Chesnokov, B.V.; Shcherbakova, E.P.; Nishanbaev, T.P. *Minerals of Burnt Dumps of the Chelyabinsk Coal Basin*; Ural Branch of RAS: Miass, Russia, 2008; pp. 1–139. (In Russian)

14. Murashko, M.N.; Pekov, I.V.; Krivovichev, S.V.; Chernyatyeva, A.P.; Yapaskurt, V.O.; Zadov, A.E.; Zelensky, M.E. Steklite, $\text{KAl}(\text{SO}_4)_2$: A finding at the Tolbachik Volcano, Kamchatka, Russia, validating its status as a mineral species and crystal structure. *Geol. Ore Depos.* **2013**, *55*, 594–600. [[CrossRef](#)]
15. Mizutani, Y. Volcanic sublimates and incrustations from Showashinzan. *J. Earth Sci. Nagoya Univ.* **1962**, *10*, 135–148.
16. Stoiber, R.E.; Rose, W.I. Fumarole incrustations at active Central American volcanoes. *Geochim. Cosmochim. Acta* **1974**, *38*, 495–516. [[CrossRef](#)]
17. Lapham, D.M.; Barns, J.H.; Downey, W., Jr.; Finkelman, R.B. Mineralogy associated with burning anthracite deposits of eastern Pennsylvania. In *Reports of the Common Wealth of Pennsylvania*; Dept. of Environmental Resources, Bureau of Topographic and Geologic Survey, Mineral Resources: Pennsylvania, PA, USA, 1980; Volume 78, pp. 1–82.
18. Tvrđý, J.; Sejkora, J. Novotvořené minerální fáze na hořícím odvalu dolu Kateřina v Radvanicích. *Uhlí Rudy Geol. Průzkum* **2000**, *7*, 19–24. (In Czech)
19. Ciesielczuk, J.; Krzykowski, T.; Misz-Kennan, M. Minerals formed by exhalation on the burning coal-waste dumps of the Upper Silesian Coal Basin, Poland. *Mineral. Spec. Pap.* **2010**, *36*, 74.
20. Košek, F.; Culka, A.; Jehlička, J. Raman spectroscopic study of six synthetic anhydrous sulfates relevant to the mineralogy of fumaroles. *J. Raman Spectrosc.* **2018**, *49*, 1–12. [[CrossRef](#)]
21. Parafiniuk, J.; Hatert, F. New IMA CNMNC guidelines on combustion products from burning coal dumps. *Eur. J. Mineral.* **2020**, *32*, 215–217. [[CrossRef](#)]
22. Bruker-AXS. *APEX2, Version 2014.11-0*; Bruker-AXS: Madison, WI, USA, 2014.
23. Sheldrick, G.M. *SADABS*; University of Goettingen: Goettingen, Germany, 2007.
24. Stoe & Cie. *X-AREA (Version 1.16) and X-RED (Version 1.22)*; Stoe & Cie: Darmstadt, Germany, 2001.
25. Stoe & Cie. *X-SHAPE, Version 1.06*; Stoe & Cie: Darmstadt, Germany, 1999.
26. Sheldrick, G.M. Crystal structure refinement with SHELXL. *Acta Crystallogr.* **2015**, *C71*, 3–8.
27. Dolomanov, O.V.; Bourhis, L.J.; Gildea, R.J.; Howard, J.A.K.; Puschmann, H. Olex2: A complete structure solution, refinement and analysis program. *J. Appl. Crystallogr.* **2009**, *42*, 339–341. [[CrossRef](#)]
28. Brese, N.E.; O’Keeffe, M. Bond-valence parameters for solids. *Acta Crystallogr.* **1991**, *B47*, 192–197. [[CrossRef](#)]
29. Manoli, J.M.; Herpin, P.; Pannetier, G. Structure cristalline du sulfate double d’aluminium et de potassium. *Bull. Soc. Chim. Fr.* **1970**, *1*, 98–101. (In French)
30. Graeber, E.J.; Rosenzweig, A. The crystal structures of yavapaiite, $\text{KFe}(\text{SO}_4)_2$, and goldichite, $\text{KFe}(\text{SO}_4)_2(\text{H}_2\text{O})_4$. *Am. Mineral.* **1971**, *56*, 1917–1933.
31. Anthony, J.W.; McLean, W.J.; Laughon, R.B. The crystal structure of yavapaiite: A discussion. *Am. Mineral.* **1972**, *57*, 1546–1549.
32. Alkemper, J.; Fuess, H. The crystal structures of NaMgPO_4 , $\text{Na}_2\text{CaMg}(\text{PO}_4)_2$ and $\text{Na}_{18}\text{Ca}_{13}\text{Mg}_5(\text{PO}_4)_{18}$: New examples for glaserite related structures. *Z. Kristal.* **1998**, *213*, 282–287. [[CrossRef](#)]
33. Krivovichev, S.V. *Structural Crystallography of Inorganic Oxysalts*; University Press: Oxford, UK, 2009.
34. Krivovichev, S.V. Comparative study of flexibilities of structural units in uranyl sulfates, chromates and molybdates. *Radiochemistry* **2004**, *46*, 434–437. [[CrossRef](#)]
35. West, D.V.; Huang, Q.; Zandbergen, H.W.; McQueen, T.M.; Cava, R.J. Structural disorder, octahedral coordination and two-dimensional ferromagnetism in anhydrous alums. *J. Solid State Chem.* **2008**, *181*, 2768–2775. [[CrossRef](#)]
36. Yogev-Einot, D.; Avnir, D. Pressure and temperature effects on the degree of symmetry and chirality of the molecular building blocks of low quartz. *Acta Crystallogr.* **2004**, *B60*, 163–173. [[CrossRef](#)]
37. Raade, G.; Mladeck, M.H.; Kristiansen, R.; Din, V.K. Kaatialaite, a new ferric arsenate mineral from Finland. *Am. Mineral.* **1984**, *69*, 383–387.
38. Mackintosh, J.B. Notes on some native iron sulphates from Chili. *Am. J. Sci.* **1889**, *38*, 242–245. [[CrossRef](#)]
39. Scordari, F. The crystal structure of ferrinatriite, $\text{Na}_3(\text{H}_2\text{O})_3[\text{Fe}(\text{SO}_4)_3]$ and its relationship to Maus’s salt, $(\text{H}_3\text{O})_2\text{K}_2\{\text{K}_{0.5}(\text{H}_2\text{O})_{0.5}\}_6[\text{Fe}_3\text{O}(\text{H}_2\text{O})_3(\text{SO}_4)_6](\text{OH})_2$. *Mineral. Mag.* **1977**, *41*, 375–383. [[CrossRef](#)]
40. Demartin, F.; Castellano, C.; Gramaccioli, C.M.; Campostrini, I. Aluminocoquimbite, $\text{AlFe}(\text{SO}_4)_3 \cdot 9\text{H}_2\text{O}$, a new aluminum iron sulfate from Grotta dell’Allume, Vulcano, Aeolian Islands, Italy. *Can. Mineral.* **2010**, *48*, 1465–1468. [[CrossRef](#)]

41. Demartin, F.; Gramaccioli, C.M.; Campostrini, I. Pyracmonite, $(\text{NH}_4)_3\text{Fe}(\text{SO}_4)_3$, a new ammonium iron sulfate from La Fossa crater, Vulcano, Aeolian Islands, Italy. *Can. Mineral.* **2010**, *48*, 307–313. [[CrossRef](#)]

Publisher’s Note: MDPI stays neutral with regard to jurisdictional claims in published maps and institutional affiliations.



© 2020 by the authors. Licensee MDPI, Basel, Switzerland. This article is an open access article distributed under the terms and conditions of the Creative Commons Attribution (CC BY) license (<http://creativecommons.org/licenses/by/4.0/>).